

A Bayesian on-off analysis of cosmic ray data

Dalibor Nosek^a, Jana Nosková^b

^aCharles University, Faculty of Mathematics and Physics, Prague, Czech Republic

^bCzech Technical University, Faculty of Civil Engineering, Prague, Czech Republic

Abstract

We deal with the analysis of on-off measurements designed for the confirmation of a weak source of events whose presence is hypothesized, based on former observations. The problem of a small number of source events that are masked by an imprecisely known background is addressed from a Bayesian point of view. We examine three closely related variables, the posterior distributions of which carry relevant information about various aspects of the investigated phenomena. This information is utilized for predictions of further observations, given actual data. Backed by details of detection, we propose how to quantify disparities between different measurements. The usefulness of the Bayesian inference is demonstrated on examples taken from cosmic ray physics.

Keywords: Bayesian inference, On-off problem, Source detection, Cosmic rays

1. Introduction

The search for new phenomena often yields data that consists of a set of discrete events distributed in time, space, energy or some other observables. In most cases, source events associated with a new effect are hidden by background events, while these two classes of events cannot be distinguished in principle. Such a search can be accomplished with an on-off measurement by checking whether the same process of a constant but unknown intensity may be responsible for observed counts in the on-source region, where a new phenomenon is searched for, and in the reference off-source region, where only background events contribute. Any inconsistency between the numbers

Email address: nosek@ipnp.troja.mff.cuni.cz (Dalibor Nosek)

of events collected in these zones, when they are properly normalized, then indicates the predominance of a source producing more events in one explored region over the other.

In this study, we focus on the problems which are often encountered when searching for cosmic ray sources while detecting rare events. Characteristics of possible sources are usually proposed based on analysis of a test set of observed data. Then, further observations are to be conducted in order to examine the presence of a source or to improve conditions for its verifications. But, due to unknown phenomena, the outcome is always uncertain which calls, first, for as less as possible initial assumptions about underlying processes and, second, for the quantification of disparities between observations with the option to correct for experimental imperfections.

In order to satisfy the first condition, we follow our previous analysis of on-off measurements formulated within the Bayesian setting [1]. Unlike other Bayesian approaches [2–9], we handle the source and background processes on an equal footing. This option provides us with solutions that are minimally affected by external presumptions. In order to track the behavior of a signal registered in a selected on-source region, we utilize variables with the capability to assess the consistency between on-off measurements. Specifically, giving the net effect, the difference variable [1] is well suited for estimating source fluxes if exposures are known. In case of stable or at least predictable background rates, we eliminate the effect of exposures by using fractional variables which reveal relatively the manifestation of a source. For example, the time evolution of a given source, if still observed in the same way, is easily examined by the ratio of the on-source rate to the total rate. In a more general case, we employ the on-source rate expressed in terms of the rate deduced from the background. In summary, we receive posterior distributions of different variables that include what is available from measurements, while providing us with all kinds of estimates, as traditionally communicated, and allowing us to make various observation-based predictions.

Related to the on-off issue, the Bayesian inference provides solutions in the case of small numbers, including the null experiment or the experiment with no background, when classical methods based on the asymptotic properties of the likelihood ratio statistic [10–13] are not easily applicable. Also, there are no difficulties with the regularity conditions of Wilks' theorem, with unphysical likelihood estimates or with the discreteness of counting experiments, in general, see e.g. Refs. [14–17]. On the other hand, the subjective nature of Bayesian reasoning, often mentioned as its disadvantage, may be

at least partially eliminated by using a family of uninformative prior options.

The proposed method is suitable for experiments searching for rare events in which the observational conditions may not be adjusted optimally, with little opportunity for repeating measurements conducted under exactly the same conditions. Besides searches for possible sources of the highest energy cosmic rays, see e.g. Refs. [18–22], examples include observations of peculiar sources which exhibit surprising temporal or spectral behavior. Another class of observations comprises searches for events accompanying radiation from transient sources that have been identified in different energy ranges. The identification of the properties of very-high-energy γ -rays associated with observed gamma-ray bursts belongs to this class of problems [1–3].

The structure of this paper is as follows. Our formulation of the Bayesian approach to the on-off problem is described in Section 2, complemented by five Appendices. Further details about our approach can be found in Ref. [1]. In Section 2.1 we summarize how to store experimental information by using appropriate on-off variables. Two ways to examine possible inconsistencies in independent observations are proposed in Sections 2.2 and 2.3. Several realistic examples taken from cosmic ray physics are presented and discussed in Section 3. The paper is concluded in Section 4.

2. Bayesian inferences from on-off experiment

In the on-off experiment, two kinds of measurements are collected in order to validate a source signal immersed in background. The number of on-source events, n_{on} , is recorded in a signal on-source region, while the number of off-source events, n_{off} , detected in a background off-source zone serves as a reference measurement. The on- and off-source counts are modeled as discrete random variables generated in two independent Poisson processes with unknown on- and off-source means, μ_{on} and μ_{off} , i.e. $n_{\text{on}} \sim \text{Po}(\mu_{\text{on}})$ and $n_{\text{off}} \sim \text{Po}(\mu_{\text{off}})$. The relationship between the on- and off-source zone is ensured by the ratio of on- and off-source exposures $\alpha > 0$.

In the Bayesian approach, for on- and off-source means we adopted a family of prior distributions conjugate to the Poisson sampling process [1]. This family consists of Gamma distributions, i.e.

$$\mu_{\text{on}} \sim \text{Ga}(s_p, \gamma_p - 1), \quad \mu_{\text{off}} \sim \text{Ga}(s_q, \gamma_q - 1), \quad (1)$$

where $s_p > 0$ and $s_q > 0$ are prior shape parameters, and the prior rate parameters $\gamma_p > 1$ and $\gamma_q > 1$. It includes several frequently discussed

options, i.e. scale invariant, uniform, as well as Jeffreys' prior distributions. After the on-off measurement has been conducted, when n_{on} and n_{off} counts were registered independently in the on- and off-source regions, using Eq.(1) we obtain independent posterior distributions

$$(\mu_{\text{on}} | n_{\text{on}}) \sim \text{Ga}(p, \gamma_p), \quad (\mu_{\text{b}} | n_{\text{off}}) \sim \text{Ga}(q, \frac{\gamma_q}{\alpha}), \quad (2)$$

where $\mu_{\text{b}} = \alpha\mu_{\text{off}}$ denotes the expected background rate in the on-source zone and $p = n_{\text{on}} + s_p$ and $q = n_{\text{off}} + s_q$. For more details see Ref. [1].

We recall that our next steps diverge from the traditional treatment. In order to assess what is observed, we define suitable on-off variables by combining the on- and off-source means, assuming that the underlying processes are independent. From the Bayesian perspective, this choice is motivated by the fact that, according to Jeffreys' rule, the joint prior distribution is separable in the on- and off-source means [1, 2]. Furthermore, as in classical statistical approaches [10–16], the proposed option allows us to obtain adequate results regardless of in which of the two zones the source effects are revealed [1, 7].

2.1. On-off variables

In our previous work [1], we focused on the properties of the difference between the on-source and background means, $\delta = \mu_{\text{on}} - \mu_{\text{b}}$, using maximally uninformative joint distributions, as dictated by the principle of maximum entropy. In this section, we briefly recapitulate our previous result and introduce other on-off variables that equally well describe the on-off problem.

Under the transformation $\delta = \mu_{\text{on}} - \mu_{\text{b}}$, with a real valued domain, while keeping $\mu_{\text{b}} = \alpha\mu_{\text{off}}$ unchanged and marginalizing over μ_{b} , the probability density function of the difference is (for details of our notation see Ref. [1])

$$f_{\delta}(x) = \frac{\gamma_p^p (\frac{\gamma_q}{\alpha})^q}{\Gamma(p)} e^{-\gamma_p x} x^{p+q-1} U(q, p+q, \eta x), \quad x \geq 0, \quad (3)$$

$$f_{\delta}(x) = \frac{\gamma_p^p (\frac{\gamma_q}{\alpha})^q}{\Gamma(q)} e^{\frac{\gamma_q}{\alpha} x} (-x)^{p+q-1} U(p, p+q, -\eta x), \quad x < 0, \quad (4)$$

where $p = n_{\text{on}} + s_p$, $q = n_{\text{off}} + s_q$, $\eta = \gamma_p + \frac{\gamma_q}{\alpha}$, $\Gamma(a)$ stands for the Gamma function and $U(a, b, z)$ is the Tricomi confluent hypergeometric function [23]. Exhaustive discussion concerning this distribution can be found in Ref. [1], where also some special cases ($\gamma_p = \gamma_q \rightarrow 1$) based on uninformative prior

distributions, scale invariant ($s_p = s_q \rightarrow 0$), Jeffreys' ($s_p = s_q = \frac{1}{2}$) and uniform ($s_p = s_q = 1$) options, are described.

The difference δ yields information about the source flux. The posterior distribution of the source flux is obtained by a scale transformation, i.e. $j = \delta/a$ where $a = \frac{\alpha}{1+\alpha}A$ is the exposure of the on-source zone and A denotes the integrated exposure of the on-off experiment, both considered as constants.

A similar picture is obtained with the ratio of the on-source and background means ($\mu_b = \alpha\mu_{\text{off}}$)

$$\beta = \frac{\mu_{\text{on}}}{\mu_b}, \quad \beta \geq 0. \quad (5)$$

This variable represents the intensity registered in the on-source region expressed in terms of the background intensity, i.e. $\beta \leq 1$ when no source is present in the on-source zone. The ratio β obeys the generalized Beta distribution of the second kind [24], $\beta \sim B_{g2}(p, q, \rho)$ where $p = n_{\text{on}} + s_p$, $q = n_{\text{off}} + s_q$ and $\rho = \alpha\gamma_p/\gamma_q$, with the probability density function

$$f_\beta(x) = \frac{\rho^p}{B(p, q)} \frac{x^{p-1}}{(1 + \rho x)^{p+q}}, \quad x \geq 0, \quad (6)$$

where $B(a, b)$ is the Beta function [23]. This posterior distribution was obtained after the transformation $\beta = \mu_{\text{on}}/\mu_b$ while treating μ_{on} and μ_b as independent variables (see Eq.(2)) and keeping μ_b unchanged, with the Jacobian $J = \mu_b$, and marginalizing over μ_b .

In a special case, using the uniform prior distributions for the on- and off-source means, i.e. $\gamma_p = \gamma_q \rightarrow 1$ and $s_p = s_q = 1$, and assuming that the on-off data were registered in the regions of the same exposure, when $\rho = \alpha = 1$, the posterior distribution for the ratio β written in Eq.(6) reduces to the result given originally in Ref. [5]. Assuming $\gamma_p = \gamma_q \rightarrow 1$ and $\alpha = 1$, i.e. $\rho = 1$, the result presented in Eq.(13) in Ref. [6] is obtained.

In some cases, it may be appropriate to use a variable

$$\omega = \frac{\mu_{\text{on}}}{\mu_{\text{on}} + \mu_{\text{off}}}, \quad \omega \in \langle 0, 1 \rangle, \quad (7)$$

that represents the fraction of the total intensity registered in the on-source zone. Considering that $\omega = \alpha\beta/(1 + \alpha\beta)$, we recover from Eq.(6) that the probability density function of the proportion ω is

$$f_\omega(x) = \frac{\kappa^p}{B(p, q)} \frac{x^{p-1}(1-x)^{q-1}}{[1 + (\kappa - 1)x]^{p+q}}, \quad x \in \langle 0, 1 \rangle, \quad (8)$$

where $p = n_{\text{on}} + s_p$, $q = n_{\text{off}} + s_q$ and $\kappa = \gamma_p/\gamma_q$ is the ratio of the prior rate parameters. In this case, equally intensive on- and off-source processes ($\mu_{\text{on}} = \mu_{\text{b}}$) are described by a balance value of $\omega = \frac{\alpha}{1+\alpha}$.

Note that any Bayesian statement based on the probabilities inferred from the above derived distributions is independent of the prior rate parameters when $\gamma_p = \gamma_q$ and thus $\rho = \alpha$. For $\gamma_p = \gamma_q$, we even have that the proportion ω obeys the Beta distribution, i.e. $\omega \sim \text{B}(p, q)$. This widely used option also follows from using the prior Beta distributions conjugate to the binomial sampling process, i.e. prior $\omega \sim \text{B}(s_p, s_q)$. In the context of on-off measurements, the classical analysis of the binomial proportion is discussed in Refs. [12, 15], for example. Point estimates of the proportion ω are traditionally used in the analysis of directional data in cosmic ray physics, see e.g. Ref. [18–20, 22, 25, 26].

The proposed Bayesian solutions to the on-off problem have other interesting features. Unlike traditional approaches [2–9], we treat the on- and off-source processes as independent. Hence, our posterior distributions are maximally noncommittal about missing information on the relationship between these processes. Moreover, receiving information separately from the on- and off-source observations, the on-off problem is examined without a predetermined assumption in which zone the source is to be searched for [1]. Thus, any detected imbalance will lead to the same conclusion notwithstanding the region where more activity is expected [1]. Note that most classical test statistics relevant to the on-off problem possess the same property [11, 15, 16].

Other technical details are summarized in Appendices. In Appendix A we show that all three on-off variables provide the same probability of the source absence in the on-source zone. Note, however, that the fractional variables β or ω , which are easier to handle, do not substitute for the difference δ .

A way how to determine the shortest credible intervals for the on-off variables is described in Appendix B. In Appendix C we show how to modify Bayesian solutions, when a source is known to be present in the on-source zone. Similar solutions are also obtained in often adopted schemes, whereby source and background parameters are treated as independent variables [2, 3, 6–9]. In Appendix D we present Bayesian solutions for cases when background rates are known with sufficient precision.

2.2. *Waiting for next events*

Current experiments collecting rare events raise interest for predictions based on previous observations. Typically, we want to know how many events

must be registered in a subsequent experiment in order to identify a given number of events in a selected on-source zone, while relying on previous data collected under the same conditions with the same instrument. This issue is solved by constructing a relevant predictive distribution.

According to previous considerations, we assume that the numbers of on- and off-source events registered in a new experiment up to and including time t are generated in two independent Poisson processes $\{N_{\text{on}}(t); t \geq 0\}$ and $\{N_{\text{off}}(t); t \geq 0\}$ with respective rates μ_{on} and μ_{off} , i.e. among others, $N_{\text{on}}(t) \sim \text{Po}(\mu_{\text{on}}t)$ and $N_{\text{off}}(t) \sim \text{Po}(\mu_{\text{off}}t)$. Hence, we know that events of the merged Poisson process $\{N(t) = N_{\text{on}}(t) + N_{\text{off}}(t); t \geq 0\}$, $N(t) \sim \text{Po}(\mu t)$ where $\mu = \mu_{\text{on}} + \mu_{\text{off}}$, arrive into the on-source zone with the probability $\omega = \mu_{\text{on}}/\mu$ independently of each other and independently of their arrival times, see e.g. Ref. [27]. Consequently, if the total number of events $n > 0$ is collected up to time t , the corresponding number of on-source events, $Y_{\text{on}} = (N_{\text{on}}(t) | N(t) = n)$, has a binomial distribution with parameters n and ω , i.e. $Y_{\text{on}} \sim \text{Bi}(n, \omega)$. We also know that the total number of events recorded until a predefined number $k > 0$ of events arrive into the on-source zone, $Y = (N(t) | N_{\text{on}}(t) = k, \text{the on-source event is the last one})$, has a shifted negative binomial distribution (waiting time distribution) with parameters k and ω , i.e. $Y \sim \text{NBi}(k, \omega)$ with support $n = k, k + 1, \dots$, see e.g. Ref. [28].

Further, we ask for the probability $p_{n,k}(\omega)$ that more than n events in total are collected before the k -th on-source event is registered if, as justified above, events are switched independently between on- and off-source zones with the probability ω . We obtain ($k > 0$ and $n = k, k + 1, \dots$)

$$p_{n,k}(\omega) = P(Y > n | \omega) = P(Y_{\text{on}} < k | \omega) = \sum_{i=0}^{k-1} \binom{n}{i} \omega^i (1 - \omega)^{n-i}, \quad (9)$$

where we use the relation between the negative binomial variable Y and the binomial variable Y_{on} , see e.g. Eq.(5.31) in Ref. [28]. This way, Eq.(9) gives the probability of the waiting time for the k -th on-source event when the time is measured in terms of the total number of collected events n .

In order to determine the chances of identifying on-source events in a new series of observations, we need to be informed about the binomial parameter ω . We use the fact that, in the Bayesian concept, the information on future measurements is contained in the posterior predictive distribution of unobserved observations, conditional on the already observed data. This distribution is obtained by marginalizing the distribution of the new data,

given parameters, over the posterior distribution of parameters, given the previous data, accounting thus for uncertainty about involved parameters.

Since the Poisson processes guarantee that the new and old observations in disjoint time intervals are independent, when conditioned on parameters μ_{on} and μ_{off} , or, equivalently, on $\mu = \mu_{\text{on}} + \mu_{\text{off}}$ and $\omega = \mu_{\text{on}}/\mu$, and since the waiting time probability given in Eq.(9) is independent of μ , we can write

$$P(Y > n, \mu, \omega | D) = P(Y > n | \omega) p(\mu, \omega | D), \quad (10)$$

where $D = (n_{\text{on}}, n_{\text{off}})$ denotes the old on-off data and $p(\mu, \omega | D)$ is the joint posterior distribution of μ and ω which is obtained via Bayes' rule using the prior distributions for μ_{on} and μ_{off} in Eq.(1). Hence, by marginalizing over μ and ω , we obtain from Eqs.(9) and (10) that, in the new data set, the waiting time for the k -th on-source event exceeds n with the probability

$$P_{n,k} = \int_0^1 \left[\int_0^\infty P(Y > n, \mu = y, \omega = x | D) dy \right] dx = \int_0^1 p_{n,k}(x) f_\omega(x) dx, \quad (11)$$

where $f_\omega(x) = p(\omega = x | D) = \int_0^\infty p(\mu = y, \omega = x | D) dy$ is the posterior distribution of the proportion ω given in Eq.(8). In particular, assuming that $\omega \sim B(p, q)$ for $\gamma_p = \gamma_q$ ($\kappa = 1$) where $p = n_{\text{on}} + s_p$ and $q = n_{\text{off}} + s_q$ are known from the previous measurement, it follows that

$$P_{n,k} = \int_0^1 p_{n,k}(x) f_\omega(x) dx = \sum_{i=0}^{k-1} \binom{n}{i} \frac{B(p+i, q+n-i)}{B(p, q)}. \quad (12)$$

Here, the Beta functions are replaced by the incomplete Beta functions, $B(a, b) \rightarrow B_{\frac{1}{1+\alpha}}(a, b)$, if a source is considered to be present in the on-source zone, see Appendix C.

The application of this result to the new data allows us to assess the consistency between subsequent observations. Consider that n new events in total are registered until the k -th new event arrives into the on-source zone, while the previous data has been processed. We know that the probability of the new observation is $P_{n,k}$ provided the new and old data are generated in the counting model described above. In the classical sense, it means that our initial assumptions are not valid at a level of confidence $\text{CL} < 1 - P_{n,k}$.

Hence, at this level of confidence, our data-driven model fails to describe what has been measured and we conclude that, besides other possibilities, the new data may indicate a smaller on-source signal or a larger background rate than would correspond to the previous measurement.

2.3. Comparison of on-off measurements

In this Section we address the question of how to compare two independent on-off measurements. Our goal is to quantify statistically which of the measurements indicate a more intense emitter, while relying on information about observations contained in the posterior distributions of on-off variables. Besides sequential measurements performed under similar conditions, we also admit experiments conducted with different equipments, for example, when different sources in different spatial, time or energy ranges are observed.

We assume that two independent on-off observations, marked by indices 1 and 2, were collected and processed by the method described in Section 2.1. Depending on what we want to examine, we choose one type of the on-off variable. The relationship between the two Bayesian outputs is quantified by the probability $P(\tau_1 < A \tau_2 | D_1, D_2)$ where τ_1 (τ_2) is a suitable on-off variable ($\tau = \delta, \beta$ or ω) for the first (second) measurement and $D_1 = (n_{\text{on}_1}, n_{\text{off}_1})$ ($D_2 = (n_{\text{on}_2}, n_{\text{off}_2})$) denotes the corresponding on-off data. This probability is determined by integrating the joint probability distribution of τ_1 and τ_2 over a relevant two-dimensional domain. Here, a constant A is used to account, at least to first order, for different observational conditions or experimental imperfections (see below).

From a practical perspective, the best way is to compare source fluxes. For this, we utilize the unconditional distributions of the differences δ_1 and δ_2 , respectively, see Eqs.(3)-(4). The probability that the flux $j_1 = \delta_1/a_1$ observed in the first observation is less than the flux $j_2 = \delta_2/a_2$ deduced from the second one, both fluxes treated as random variables, is

$$P(j_1 < j_2) = P(\delta_1 < \frac{a_1}{a_2} \delta_2) = \int_{-\infty}^{\infty} f_{\delta_1}(x_1) \left[\int_{\frac{a_2}{a_1} x_1}^{\infty} f_{\delta_2}(x_2) dx_2 \right] dx_1. \quad (13)$$

Here, the assessment of stability of source fluxes requires the knowledge of the on-source exposures, a_1 and a_2 . However, they may be affected by various imperfections associated with details of detection and data processing, especially when different sources are examined by different techniques.

The discrepancy between two independent observations can also be described by comparing the ratio variables while canceling out the effect of exposures. If we adopt the unconditional distributions for the ratio variables β_1 and β_2 given in Eq.(6), the inconsistency between two sets of on-off data can be quantified by the probability

$$P(\beta_1 < \xi\beta_2) = \int_0^\infty f_{\beta_1}(x_1) \left[\int_{\xi^{-1}x_1}^\infty f_{\beta_2}(x_2) dx_2 \right] dx_1. \quad (14)$$

Here, for further possible applications, we introduced a parameter $\xi > 0$, allowing us to compare multiples of the ratio variables. In a first order approach, this parameter can be employed to eliminate imperfections attributable to detection and data evaluation.

When two measurements collected in the same on- and off-source zones are studied ($\alpha_1 = \alpha_2$), the proportion ω is advantageously used after a straightforward modification of Eq.(14). Note also that the proposed probabilities are easily modified if sources are assumed to be present in their on-source zones, see Appendix C. Specifically, when non-negative source rates are guaranteed due to external arguments, the probabilities of inconsistency are obtained by putting the conditional distributions into the relevant equations while changing the integration limits accordingly.

The integration in Eqs.(13) and (14) is to be performed numerically over the indicated two-dimensional sets. In some counting experiments, background rates can be estimated with sufficient accuracy from auxiliary measurements or modeled numerically. With this simplification, we obtained explicit formulae for the probabilities of inconsistency summarized in Appendix E.

The probabilities of inconsistency given in Eqs.(13) and (14) have somewhat different meanings. The difference δ allows us to quantify disparities between source fluxes, when on-source exposures are known. The probabilities based on the fractional variables β and ω describe discrepancies between on-source observations when expressed with respect to the background or total measurements, respectively. Thus, in more complicated cases, additional information about details of detection and data processing is needed for their correct interpretation (e.g. background rates, energy ranges, data quality limits etc.).

The probabilities written in Eqs.(13) and (14) do not substitute for the

probabilities of the source presence in the on-source zone, see Appendix A. Indeed, it can be more likely that a larger flux is observed from a source which is found to be less significant than the other, i.e. $P(j_1 < j_2) > 0.50$ while $P_1^+ > P_2^+$ and vice versa. Note also that quantified disparities between source fluxes, $P(j_1 < j_2)$, when compared to ratio results, $P(\beta_1 < \beta_2)$, for a given pair of observations, may reveal hitherto unnoticed features that could affect measurements, were not considered during data processing or disrupted homogeneity of the underlying Poisson processes.

3. Examples

The usefulness of the method described in Section 2 is demonstrated using arrival directions of the highest energy cosmic rays measured by the Pierre Auger Observatory [20–22]. Considering a predefined set of positions of nearby active galactic nuclei (AGN), we provide information to what extent is this set of possible sources related to directional data after this association has been suggested [18, 19]. In a similar way, we also examine a signal that has been initially associated with the region around Centaurus A (Cen A) [20, 21]. We emphasize that earlier conclusions [18–22] are in line with our analysis. Our aim is not to reassess previous studies, we only point out how the previous findings may be viewed from different perspectives.

Regardless of the results of further analysis [20, 22], we assumed that the signals from AGNs [18, 19] and Cen A [20, 21] have not yet been confirmed. Given the data that were observed in the preselected on-off regions, we calculated the posterior distributions of the difference and fractional variables. We assumed the same prior distributions for the on- and off-source means with common shape parameters and zero rate parameters, i.e. $s = s_p = s_q$ and $\gamma = \gamma_p = \gamma_q \rightarrow 1$. Furthermore, we derived the posterior distributions of the source flux j using $j = \delta/a$ where $a = \frac{\alpha}{1+\alpha}A$ and A denotes the integrated exposure of the period of data taking.

In the following, we show how the three on-off variables can be used when examining the previously suggested associations. Based on the results of Section 2.2, we provide examples related to the issue of waiting for the next on-source events. We also present examples of how to compare various independent measurements, see Section 2.3. In the latter case, we include the latest hot spot (HS) data obtained by the Telescope Array surface detector [29].

Table 1: AGN and Cen A data measured by the Auger surface detector [20–22] and the HS data detected by the Telescope Array [29]. Source assignment, period, exposure A in $\text{km}^2 \text{sry}$, measured on- and off-source counts and the on-off parameter α are listed in the first sixth columns. The endpoints of examined periods are denoted by $A = (\text{May } 27, 2006)$, $B = (\text{Aug } 31, 2007)$, $C = (\text{Dec } 31, 2009)$, or $C = (\text{Jan } 1, 2010)$ for Cen A, and $D = (\text{Mar } 31, 2014)$, respectively. For the HS we used the two-year data collected from $E = (\text{May } 5, 2013)$ to $F = (\text{May } 11, 2015)$, see Table 1 in Ref. [29]. The Bayesian probabilities of no source (P^-), corresponding significances (S_B) and Li-Ma significances (S_{LM}) are given in the next three columns. For Bayesian results, Jeffreys’ prior distributions were adopted, i.e. $s = \frac{1}{2}$ and $\gamma \rightarrow 1$.

Data	Period	A	n_{on}	n_{off}	α	P^-	S_B	S_{LM}
AGN	$A-B$	4500	9	4	0.266	$8.2 \cdot 10^{-5}$	3.77	3.73
AGN	$A-C$	15980	21	34	0.266	$1.7 \cdot 10^{-3}$	2.93	2.90
AGN	$A-D$	47363	41	105	0.266	$2.0 \cdot 10^{-2}$	2.05	2.03
Cen A	$C-D$	31383	3	76	0.047	0.59	-0.22	-0.31
HS	$E-F$		5	32	0.075	$7.0 \cdot 10^{-2}$	1.48	1.40

3.1. Active galactic nuclei

Among other important results [22], one of the topics of discussion regarding the distributions of arrival directions of the highest energy cosmic rays has focused on their association with a set of positions of nearby objects from the 12th edition of quasars and AGNs [30]. An initially revealed signal [18, 19] has been reinvestigated in subsequent studies using the newly registered data [20, 22].

In order to document the uses and advantages of the Bayesian reasoning, we examined data registered by the surface detector of the Pierre Auger Observatory since May 27, 2007 up to March 31, 2014 (see Table A1 in Ref. [22]), after the AGN signal was recognized [18, 19]. Specifically, we used events with energies in excess of 53 EeV and with zenith angles not exceeding 60° . For the association of the selected events with the nearby AGNs we accepted a set of parameters as defined in Refs. [18, 19] and then slightly modified [20, 22]. A complex AGN source consists of a unification of

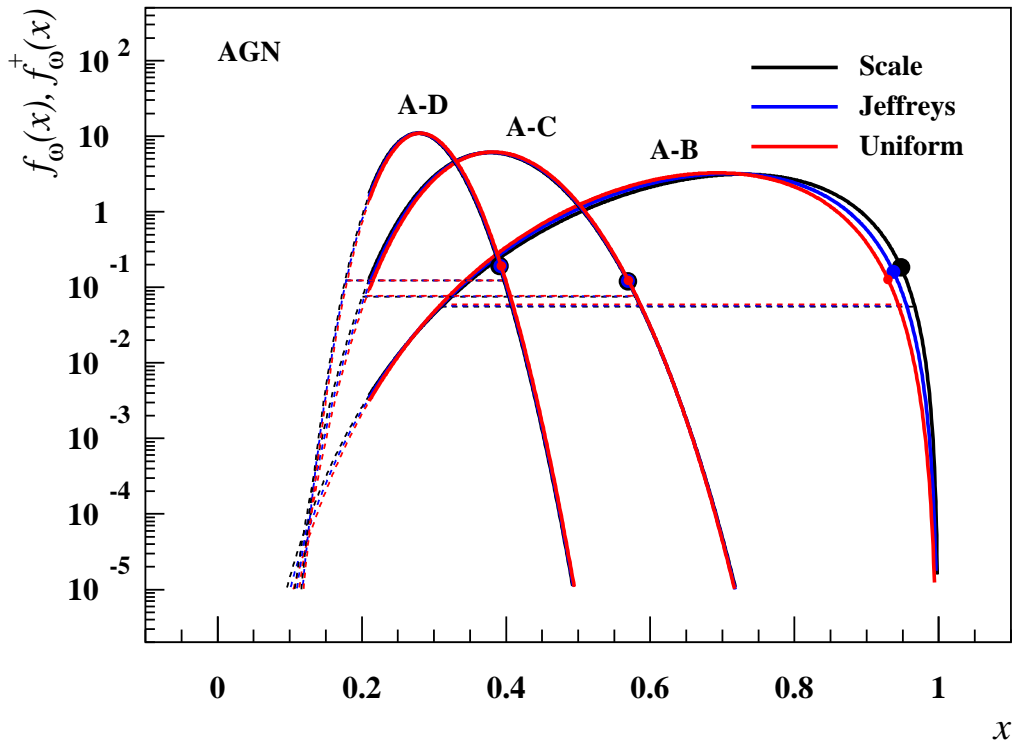


Figure 1: Distributions of proportion ω for AGN data [22]. The same uninformative priors for on- and off-source means ($s = s_p = s_q$ and $\gamma_p = \gamma_q \rightarrow 1$) are used. Results for scale invariant ($s \rightarrow 0$), Jeffreys' ($s = \frac{1}{2}$) and uniform ($s = 1$) priors are shown in black, blue and red, respectively. Distributions for the proportion, $f_\omega(x)$, and distributions $f_\omega^+(x)$, when conditioned on a non-negative source rate ($\omega \geq \frac{\alpha}{1+\alpha}$), are depicted as dashed and thick full curves, respectively. Horizontal dashed lines visualize credible intervals for the proportion ($\langle \omega_-, \omega_+ \rangle$) at a 3σ level of confidence. Upper limits at the same confidence level for the proportion assumed to be non-negative (ω_+^+ for $\omega \geq \frac{\alpha}{1+\alpha}$) are shown by colored points.

circular zones with angular radii 3.1° around the positions of AGNs within 75 Mpc (redshifts $z \leq 0.018$) [30].

We examined three sets of data collected successively, as reported in Refs. [20, 22]. Namely, we analyzed arrival directions of events registered since May 27, 2006 up to August 31, 2007 (here denoted as period *A-B*, II in Ref. [20]), up to December 31, 2009 (here *A-C*, II+III in Ref. [20]) and, finally, up to March 31, 2014 (here *A-D*, see also Ref. [22]). The integrated exposures of the Auger surface detector, measured counts of on- and

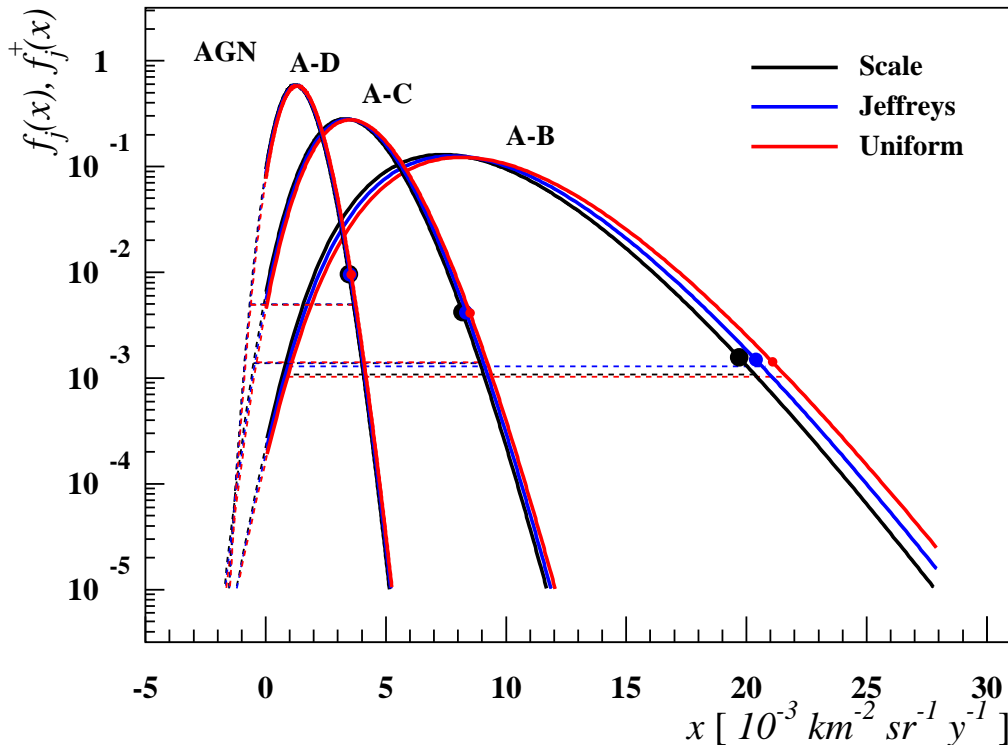


Figure 2: Distributions of source flux $j = \delta/a$ ($a = \frac{\alpha}{1+\alpha}A$) for AGN data [22]. Both types of distributions are shown, $f_j(x)$ (dashed curves) and $f_j^+(x)$ for $j \geq 0$ (thick full curves). For further details see caption to Fig.1.

off-source events and on-off parameters α , all taken from Refs. [20, 22], are summarized in the first six columns in the upper three lines in Table 1. In this table, we also show some statistical characteristics based on the Jeffreys' priors ($s = \frac{1}{2}$, $\gamma \rightarrow 1$) and asymptotic Li-Ma significances [11].

The posterior distributions for the proportion ω are depicted in Fig.1. In this figure, we show results with three kinds of uninformative prior distributions, namely, for scale invariant ($s \rightarrow 0$, in black), Jeffreys' ($s = \frac{1}{2}$, blue) and uniform ($s = 1$, red) prior distributions. Two families of posterior distributions are depicted, unconditional distributions (dashed curves) as well as distributions conditioned on a non-negative source rate in the on-source region (thick full lines), i.e. assuming $\omega \geq \frac{\alpha}{1+\alpha}$, see Appendix C. In Fig.1, also credible intervals and upper limits for the proportion ω at a 3σ level of confidence are visualized (see Appendix B).

As an alternative, in Fig.2 we show posterior distributions for the AGN

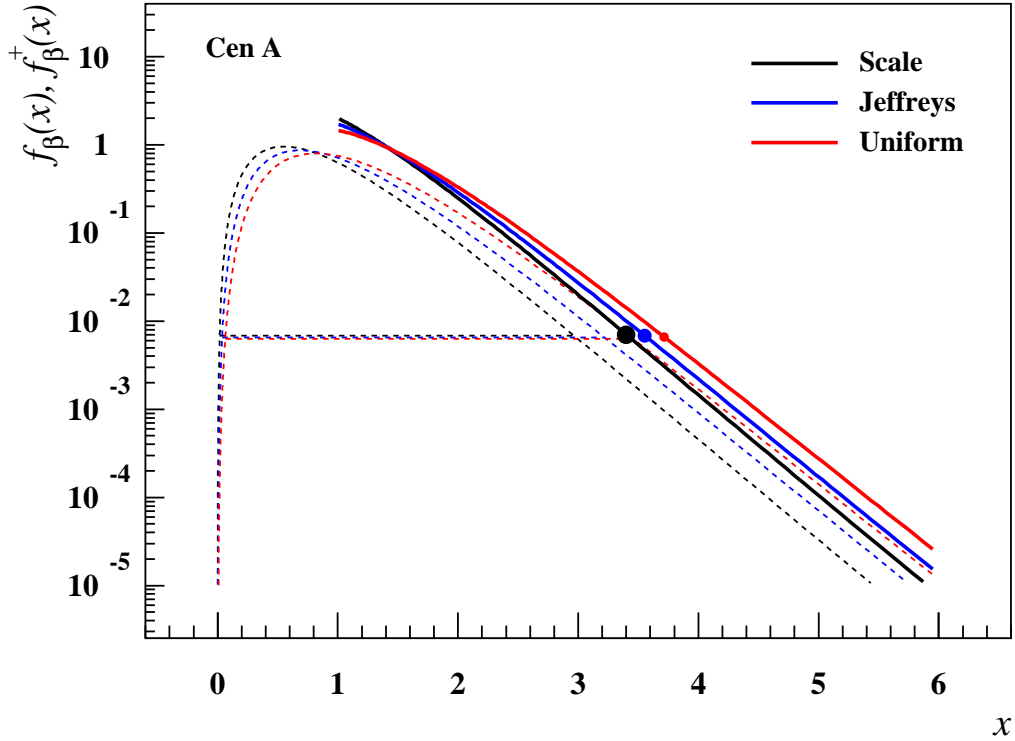


Figure 3: Distributions of ratio β for Cen A data [22]. Both types of distributions are shown, $f_\beta(x)$ (dashed curves) and $f_\beta^+(x)$ for $\beta \geq 1$ (thick full curves). For further details see caption to Fig.1.

flux $j = \delta/a$, given the on-off data in three examined period, and again using the three uninformative prior options. Relevant credible intervals at a 1σ level of significance are depicted in Fig.4 as functions of the common shape parameter. The classical estimates [16] and the results with known background rates (see Appendix D) are also shown in Fig.4.

The posterior distributions shown in Figs.1 and 2 clearly illustrate that the Bayesian inferences are only slightly dependent on the choice of uninformative prior distributions ($s \in \langle 0, 1 \rangle$, $\gamma \rightarrow 1$) if the AGN source exhibits a sufficiently high activity, see also Fig.4. In such cases, due to large probabilities of the source presence in the AGN region, all conditional distributions approximately follow in their domains relevant unconditional distributions. Furthermore, we learned how accessible information about the AGN source evolves with an increasing number of events recorded in the three successive sets of on-off data. Our Bayesian estimates agree with the reported fractions

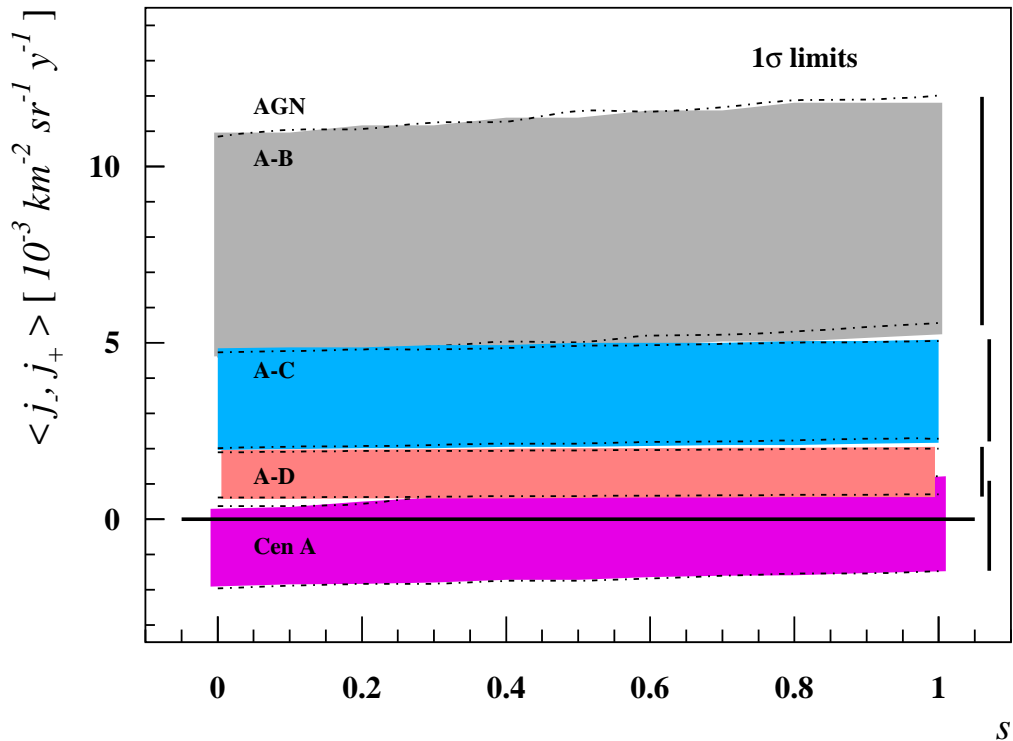


Figure 4: Credible intervals for source flux $j = \delta/a$ ($a = \frac{\alpha}{1+\alpha}A$) at a 1σ level of confidence are shown as functions of the common shape parameter of prior distributions $s = s_p = s_q$ ($\gamma_p = \gamma_q \rightarrow 1$). Results for AGN (gray, blue and red bands) and Cen A (magenta) data [22] are depicted. Dashed-dot lines indicate limits estimated using the approach based on known background (see Appendix D). Black vertical lines show classical limits deduced within the unbounded profile likelihood analysis [16]. The horizontal black line represents the background expectation.

of events associated with the AGN region and their downward trend [20, 22].

A decreasing AGN signal is also reflected in the predictions of the waiting time for the next on-source events when compared with future observations, see Section 2.2. In Fig.5, we show the probability that less than a given number of AGN events were detected in a number of subsequent measurements, while relying on previous observations. For example, the Auger data collected in *A-B* period predicts that a total of 42 events should be registered prior to the next 12 AGNs events with a probability below $4 \cdot 10^{-3}$ (black lines). Hence, when confronted with the Auger data from *B-C* period, in which these numbers were observed, such a waiting time is very unlikely.

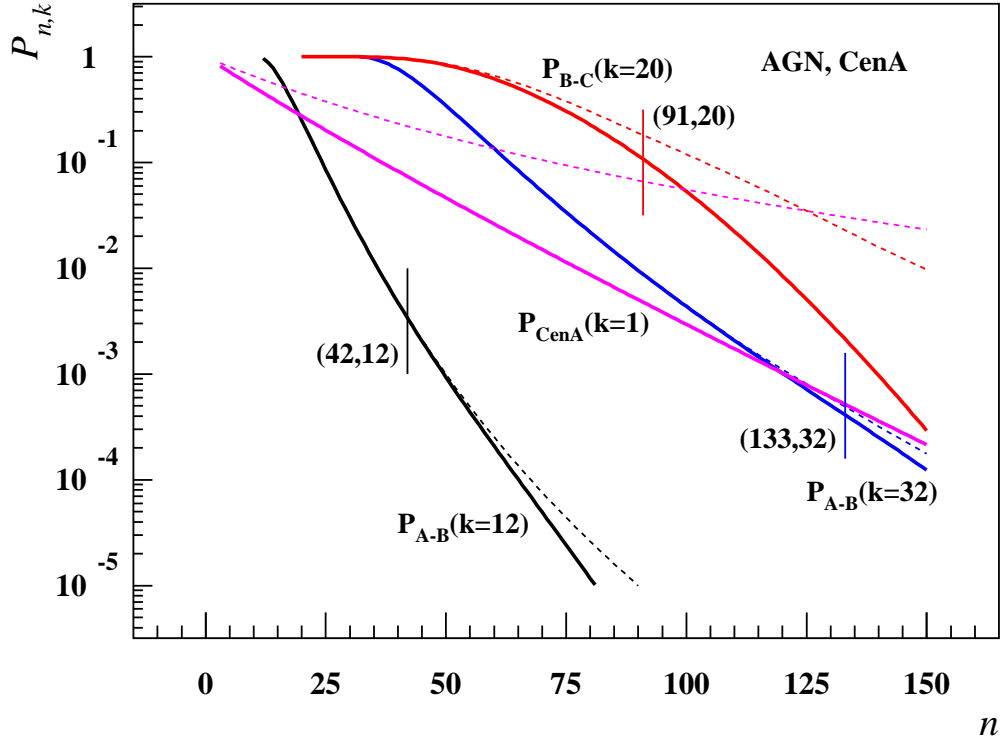


Figure 5: Waiting time predictions. The probabilities $P_{n,k}$ that less than k on-source events are observed are shown as functions of the total number of registered events n . Predictions based on the AGN signals observed in A - B period for the next 12 (32) AGN events are shown in black (blue). B - C predictions for the next 20 AGN counts are in red. Magenta lines are for predictions of one next Cen A event, based on the Cen A data from C - D period. Dashed (full) lines show unconditional (conditional) results based on Jeffreys' prior distributions. Colored vertical lines indicate observations of (n, k) events collected in the subsequent AGN periods.

This result allows us to conclude that the B - C data is inconsistent with the A - B observation at about a 3σ level of confidence.

Independent AGN observations are compared in Fig.6, see Section 2.3. In this case, the source fluxes as well as the ratios $\beta(\xi \approx 1)$ are well suited since still the same on- and off-source zones are observed with the same instrument. The parameter ξ is employed to show the probability that one ratio is ξ -times smaller than the other or it can correct for imperfections, if known (e.g. different background rates, energy ranges, seasonal effects etc.). Our results depicted in Fig.6 agree with the findings drawn from the waiting

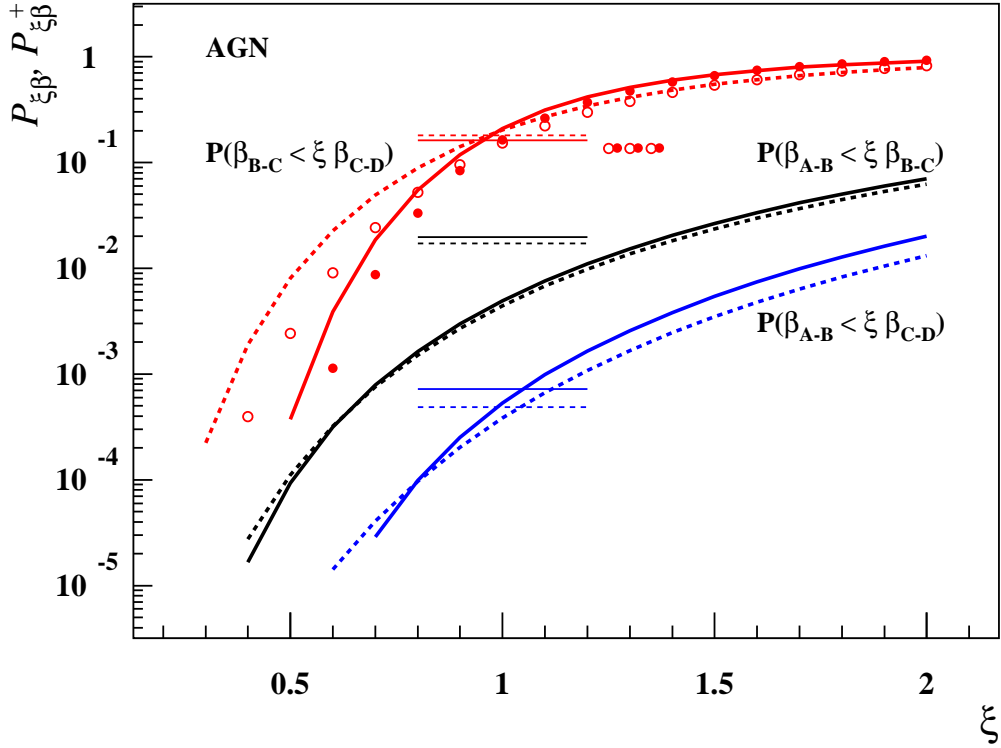


Figure 6: Probabilities of inconsistency for the ratio β , $P_{\xi\beta} = P(\beta_1 < \xi\beta_2)$, deduced from the AGN data are shown as functions of the parameter ξ (see Section 2.3). Black, blue and red lines are for the comparison of three separated AGN periods. Dashed and full lines show unconditional ($P_{\xi\beta}$) and conditional ($P_{\xi\beta}^+$) results, respectively, based on Jeffreys' priors. Red empty (full) points show unconditional (conditional) results for B - C and C - D periods assuming known background rates (see Appendix D) and uniform priors for on-source means. Thin horizontal lines indicate the probabilities of inconsistency, $P(j_1 < j_2)$, between AGN fluxes. Horizontal chains of three red points are for source fluxes provided that background rates are known (see Appendix E).

time analysis. Namely, it is very unlikely that the AGN ratio from A - B period is less than the ratios derived from the two subsequent periods, and the same holds for the fluxes (black and blue results). But the probability of inconsistency between B - C and C - D periods are much larger (red results). Note also that the discrepancy between the probabilities calculated for the AGN fluxes and ratios, when relating A - B and B - C periods for $\xi \approx 1$ (in black), may indicate inhomogeneities of the underlying Poisson processes.

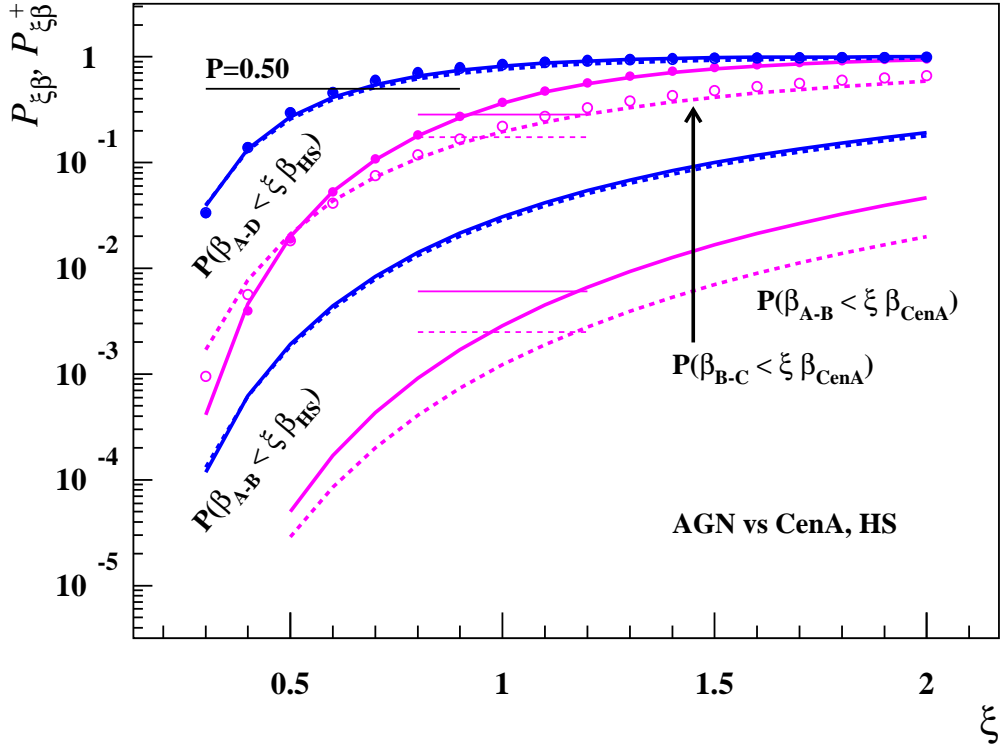


Figure 7: Probabilities of inconsistency for the ratio β are shown as functions of the parameter ξ (see Section 2.3). The AGN data collected in periods A - B and B - C are compared to the Cen A signal in period C - D , see magenta lines. The probabilities that quantify inconsistency between the HS signal and the AGN data registered in periods A - B and A - C are shown in blue. The black horizontal line indicates a probability of 0.50. For further details see caption to Fig.6.

We also examined two possible signals deduced from different on-off measurements that were collected by different experiments. In Fig.7, the two-years HS data collected on the northern hemisphere by the Telescope Array surface detector (see Table 1 in Ref. [29]) is compared to the AGN signal measured by the Auger surface array on the southern hemisphere [20, 22]. Using two sets of the AGN data, A - B and A - D periods, the probabilities of inconsistency for the ratio β are shown as functions of the parameter ξ (blue lines). Interestingly, since $P(\beta_{A-D} < \xi\beta_{HS}) > 0.70$ for $\xi \approx 1$, it is more likely that the less visible HS source ($S_B = 1.48$, see Table 1) manifests itself more markedly, when confronted with background, than the latest signal from AGN emitters (A - D period) which are more easily identified ($S_B = 2.05$,

see Table 1). In this example, the parameter ξ may be utilized to correct for different energy scales ($E \geq 55$ EeV for the HS [29] while $E > 53$ EeV for the AGNs [22] plus systematic uncertainties) and for different background fluxes (at these energies, the overall flux on the northern hemisphere was measured to be at least twice as large as the southern flux, see e.g. Ref. [31]). If the northern background is truly larger than the southern one and, consequently, the observation of the HS signal is more difficult, one can correct for this effect by using $\xi > 1$, enlarging even more the probability that the AGNs are weaker emitters.

3.2. Centaurus A

Centaurus A (NGC 5128), located at a distance less than 4 Mpc, is known as a promising candidate source of the highest energy cosmic rays. Moreover, the nearby Centaurus cluster with large concentration of galaxies lies in approximately the same direction, at a distance of about 50 Mpc. The excess of the highest energy events found in the vicinity of Cen A and the properties of observed signal have been originally reported in Ref. [20]. However, this observation was not confirmed in successive measurements [22].

In this example, we show how the disappearance of a previously specified signal [20] can be justified by using subsequently collected data within the Bayesian analysis. We adopted the data registered by the surface detector of the Pierre Auger Observatory since January 1, 2010 up to March 31, 2014 [22] (here period *C-D*), after the original Cen A signal was identified [20]. The arrival directions of events with energies above 53 EeV and zenith angles up to 60° were taken from Table A1 in Ref. [22]. Based on the previous findings [20], we assumed a circular region with an angular radius of 18° , located around the position of Cen A ($\alpha = 201.4^\circ, \delta = -43.0^\circ$). The basic characteristics of the Cen A region and the numbers of events collected in the examined period are summarized in the last but one row in Table 1.

In Fig.3, we give an example of most unbiased information on the highest energy cosmic rays associated with the preselected Cen A zone, which can be derived from the latest data [22]. In this figure, the posterior distributions for the ratio β and corresponding credible intervals at a 3σ level of confidence are shown for three kinds of uninformative prior distributions. We distinguish for unconditional distributions ($\beta \geq 0$) and distributions conditioned on a non-negative source rate in the on-source region ($\beta \geq 1$.) Credible intervals for the source fluxes j at a 1σ level of confidence are depicted in Fig.4 as functions of the common shape parameter $s \in \langle 0, 1 \rangle$ ($\gamma \rightarrow 1$).

The Bayesian inference indicates that the presence of the source in the originally selected Cen A region is less likely than its absence therein when observations since 2010 are considered, i.e. $P^- \geq 0.50$ ($S_B \leq 0$) for almost all prior options, for the Cen A flux see Fig.4. This conclusion agrees with the classical results based on asymptotic techniques, see Table 1. Hence, the conditional distributions for the ratio β , $f_\beta^+(x)$ shown in Fig.3, poorly reflect reality.

The absence of the signal registered in the Cen A region in the latest observation can be quantified using the waiting time for one next Cen A event, see Section 2.2. It is found in a marked difference between unconditional and conditional predictions that disqualifies the latter option, see Fig.5. Based on this data, over fifty events should be needed in order that the new one was identified in the Cen A region at a 90% level of confidence. Using the method of Section 2.3, the same is documented in Fig.7. Namely, it is more likely that the four-years Cen A signal is weaker than the AGN activity measured in two preceding periods (magenta results). Here, the parameter ξ can account for different background zones of Cen A and AGNs emitters and different shapes of their energy spectra, for example.

In this regard, it is worth recalling that the Auger collaboration has lately pointed out that the significance of the excess of events in the angular windows and energy range, as examined in this study, is less than its originally observed value [22]. This was obtained by using a broader set of data collected between January 1, 2004 and March 31, 2014, including events with zenith angles up to 80° , when the hypothesis of isotropy was tested. The most significant departure from isotropy in the available set of data was reported for events with energies beyond 58 EeV and with arrival directions within a circle of an angular radius of 15° centered on Cen A [22].

4. Conclusions

We focused on the search for new phenomena, when all relevant characteristics of a source which is suspected of causing observed effects cannot be set in an optimal way. The issue was dealt with in the context of on-off measurements assuming registration of small numbers of events that obey Poisson distributions. For this purpose, the Bayesian way of reasoning was utilized. This approach is not only statistically well justified and intuitively easily interpretable, but also provides readily computable results.

We examined three appropriately chosen on-off variables that store information available from the on-off experiment. In addition to traditionally presented results, we proposed how to utilize observation-based information for predictions and comparisons, focusing on quantification of signal stability.

By using successive measurements, increasing sets of the highest energy events collected at the Pierre Auger Observatory were examined. For comparison, also directional data reported by the Telescope Array was considered. Using the recent Auger observations, we summarized the outputs accessible in the proposed approach. We discussed the extent to which the comparison of on-off measurements may help when searching for cosmic ray sources.

Acknowledgments: We would like to acknowledge and thank our colleagues from the Pierre Auger Collaboration for many helpful discussions and, especially, for the tremendous work with data, its analysis and interpretation from which we benefit. We thank anonymous reviewer for valuable comments and suggestions that helped us improve the presentation of this paper. This work was supported by the Czech Science Foundation grant 14-17501S. The research of J.N. was partly supported by the Czech Science Foundation under project GACR P103/12/G084.

Appendix A. Source detection

Using the posterior distribution for the difference, see Eqs.(3) and (4), the probability for the absence of a source in the on-source region is [1]

$$P^- = I_{\frac{\rho}{1+\rho}}(p, q), \quad (\text{A.1})$$

where $p = n_{\text{on}} + s_p$, $q = n_{\text{off}} + s_q$, $\rho = \alpha\gamma_p/\gamma_q$ and $I_x(a, b)$ denotes the regularized incomplete Beta function [23]. Using other on-off variables, we obtain after straightforward calculations

$$P^- = P(\tau \leq \lambda_\tau) = \int_{-\infty}^0 f_\delta(x) dx = \int_0^1 f_\beta(x) dx = \int_0^{\frac{\alpha}{1+\alpha}} f_\omega(x) dx, \quad (\text{A.2})$$

where $\tau = \delta, \beta, \omega$, while $\lambda_\tau = 0, 1, \frac{\alpha}{1+\alpha}$ denotes the balance value for the difference, ratio and proportion, respectively. The probability of the presence of a source in the on-source zone is $P^+ = 1 - P^-$. When viewed in terms

of a normal variate with zero mean and unit variance, the probability P^- is converted to a Bayesian significance S_B .

Appendix B. Credible intervals

For the shortest credible interval, $\langle \tau_-, \tau_+ \rangle$, that contains the on-off variable with a probability P , one has to solve numerically ($\tau = \delta, \beta, \omega$)

$$P = \int_{\tau_-}^{\tau_+} f_\tau(x) dx, \quad f_\tau(\tau_-) = f_\tau(\tau_+), \quad (\text{B.1})$$

under the indicated condition on endpoints of the corresponding probability density function $f_\tau(x)$. An upper bound for the source intensity, τ_+ , is determined numerically using the integral in Eq.(B.1) where we put $\tau_- \rightarrow -\infty, 0$ or 0 for $\tau = \delta, \beta$ or ω , respectively, and relax the indicated limitation on endpoints of $f_\tau(x)$. For a non-negative source intensity ($\mu_{\text{on}} \geq \mu_{\text{b}}$), see Appendix C, credible intervals are derived by putting $f_\tau(x) \rightarrow f_\tau^+(x)$ into Eq.(B.1) while we set $0, 1$ or $\frac{\alpha}{1+\alpha} \leq \tau_- < \tau_+ < +\infty, +\infty$ or 1 , respectively. For upper bounds for a known source we set directly $\tau_- = 0, 1$ or $\frac{\alpha}{1+\alpha}$ and relax the limitation on endpoints of $f_\tau^+(x)$.

Appendix C. Known source

In a variety of problems we know with certainty that an active source is present in the on-source region or at least we have a good indication that it may be assumed. This issue is encountered when searching for accompanying radiation from already identified emitters, for example. When the mean event rate in the on-source zone can only increase beyond what is expected from background, the corresponding probability distributions are derived conditioning on the non-negative values of the difference of the on-source and background means, i.e. $\mu_{\text{on}} \geq \mu_{\text{b}} = \alpha\mu_{\text{off}}$ or, alternatively, $\tau \geq \lambda_\tau$ where $\tau = \delta, \beta, \omega$ and $\lambda_\tau = 0, 1, \frac{\alpha}{1+\alpha}$ for the difference, ratio and proportion, respectively. For the conditional distributions we have

$$f_\tau^+(x) = f_\tau(x | x \geq \lambda_\tau) = \frac{f_\tau(x)}{P^+}, \quad x \geq \lambda_\tau, \quad (\text{C.1})$$

where the Bayesian probability of the presence of a source in the on-source zone, $P^+ = 1 - P^- = I_{\frac{1}{1+\rho}}(q, p)$, follows from Eq.(A.1). Note that if the

probability P^+ approaches one, when it is exceedingly likely that the source contributes to the intensity detected in the on-source zone, the on-off problem is well described in the unconditional regime, since $f_\tau^+(x)$ tends to $f_\tau(x)$ in the domain where $x \geq \lambda_\tau$.

We recall that, by this construction, we obtain results which were derived in another way [2, 3, 6–9], assuming that the source and background rates are non-negative, i.e. $\mu_s = \mu_{\text{on}} - \mu_b \geq 0$ and $\mu_b = \alpha\mu_{\text{off}} \geq 0$, for more information see Ref. [1]. Specifically, in the context of the on-off problem, the use of the proportion ω with the Jeffreys' prior distributions was advocated in Ref. [8]. In our scheme, substituting the corresponding parameters ($p = n_{\text{on}} + \frac{1}{2}$, $q = n_{\text{off}} + \frac{1}{2}$ and $\gamma_p = \gamma_q \rightarrow 1$) into Eqs.(8) and (C.1), the posterior ω -distribution written in Eq.(27) in Ref. [8] is recovered.

Appendix D. Known background

The probability distributions of examined variables are further simplified in the case of a known background. Such a simplification may be used, for example, when searching for sources of cosmic rays in a small on-source region ($0 < \alpha \ll 1$) complemented by a much larger off-source zone which is comprised of the remaining part of the sky within the field of view of the experiment, where $n_{\text{off}} \gg 1$. Then, the number of background events observed in the on-source zone follow approximately the Poisson distribution with an estimated mean parameter $\mu_b = \alpha\mu_{\text{off}} \approx \alpha n_{\text{off}}$, since its estimated variance is negligible, $\sigma^2(\alpha n_{\text{off}}) \approx \alpha^2 n_{\text{off}} \ll \mu_b^2$. Another example is the analysis of a counting experiment that utilizes a constant background rate estimated based on modeling considerations.

In such a case, we easily obtain $\mu_{\text{on}} = (\delta + \mu_b) \sim \text{Ga}(p, \gamma_p)$ [1] and the ratio $\beta = (\mu_{\text{on}}/\mu_b) \sim \text{Ga}(p, \gamma_p\mu_b)$, where $p = n_{\text{on}} + s_p$. The proportion is given by the transformation $\omega = (\alpha\beta)/(1 + \alpha\beta)$. In summary, the probability density functions of all on-off variables are, respectively,

$$h_\delta(x) = \frac{\gamma_p^p}{\Gamma(p)} (x + \mu_b)^{p-1} e^{-\gamma_p(x + \mu_b)}, \quad x \geq -\mu_b, \quad (\text{D.1})$$

$$h_\beta(x) = \frac{(\gamma_p\mu_b)^p}{\Gamma(p)} x^{p-1} e^{-\gamma_p\mu_b x}, \quad x \geq 0, \quad (\text{D.2})$$

and

$$h_\omega(x) = \frac{(\gamma_p\mu_{\text{off}})^p}{\Gamma(p)} \frac{x^{p-1}}{(1-x)^{p+1}} e^{-\frac{\gamma_p\mu_{\text{off}}x}{1-x}}, \quad x \in (0, 1). \quad (\text{D.3})$$

In addition, assuming non-negative source rate in the on-source region, $\mu_{\text{on}} \geq \mu_{\text{b}}$ (i.e. $\delta \geq 0$, $\beta \geq 1$ or $\frac{\alpha}{1+\alpha} \leq \omega \leq 1$), we have for the corresponding probability density functions

$$h_{\tau}^{+}(x) = \frac{h_{\tau}(x)}{R^{+}}, \quad x \geq \lambda_{\tau}, \quad (\text{D.4})$$

where $\tau = \delta, \beta, \omega$, while $\lambda_{\tau} = 0, 1, \frac{\alpha}{1+\alpha}$, and R^{+} is the probability of the presence of a source in the on-source region provided a constant background mean is used¹, i.e.

$$R^{+} = \int_0^{\infty} h_{\delta}(x) dx = \int_1^{\infty} h_{\beta}(x) dx = \int_{\frac{\alpha}{1+\alpha}}^1 h_{\omega}(x) dx = \frac{\Gamma(p, \gamma_p \mu_{\text{b}})}{\Gamma(p)}, \quad (\text{D.5})$$

where $\Gamma(a, x) = \int_x^{\infty} t^{a-1} e^{-t} dt$ is the upper incomplete Gamma function. It is

useful to know that $R^{+}(p, x) = \frac{\Gamma(p, x)}{\Gamma(p)} = e^{-x} \sum_{k=0}^{p-1} \frac{x^k}{k!}$ for integer values of p .

Notice that for $\gamma_p \rightarrow 1$, $R^{-} = 1 - R^{+}$ is the p -value obtained in the classical framework, when the background hypothesis (i.e. $\mu_{\text{on}} \leq \mu_{\text{b}}$) is tested against the alternative of a source presence in the on-source zone ($\mu_{\text{on}} > \mu_{\text{b}}$) for the Poisson sampling process [15].

Appendix E. Comparison with known backgrounds

When fluctuations in the background are completely disregarded, see Appendix D, the probabilities of inconsistency introduced in Section 2.3 can be expressed explicitly. We assume two independent observations, marked by indices 1 and 2. If only non negative integer values of relevant shape parameters (s_{p_1} and s_{p_2}) are considered, the integration in Eq.(14) is easily performed using the posterior distributions given in Eq.(D.1). Then, the probability of inconsistency between source fluxes when the on-source exposures (a_1 and a_2) are known, see Eq.(13), can be written in a compact formula

¹ Note that there are typographical errors in Eqs.(26) and (27) in Ref. [1]. There should be $\Gamma(p, \gamma_p \mu_{\text{b}})$ instead of $\Gamma(p, \mu_{\text{b}})$.

$$(p_1 = n_{\text{on}_1} + s_{p_1}, p_2 = n_{\text{on}_2} + s_{p_2}, p_1, p_2 \in N)$$

$$P(j_1 < j_2) = \frac{e^{-u} v^{p_2}}{(1+v)^{p_1+p_2}} \sum_{k=1}^{p_2} \sum_{i=k}^{p_2} \binom{p_1+p_2-i-1}{p_2-i} \frac{u^{i-k}}{(i-k)!} \left(\frac{1+v}{v}\right)^i R_i(v). \quad (\text{E.1})$$

Here, $u = \gamma_{p_2} \mu_{b_2} - v \gamma_{p_1} \mu_{b_1} \geq 0$ depends on the known background rates, μ_{b_1} and μ_{b_2} , $v = (\gamma_{p_2} a_2) / (\gamma_{p_1} a_1)$ depends on the ratio of two on-source exposures, γ_{p_1} and γ_{p_2} denote the prior rates of the on-source means and $R_i(v) = 1$ for the unconditional δ -distributions given in Eq.(D.1), while

$$R_i(v) = \frac{R^+(p_1+p_2-i, (1+v)\gamma_{p_1}\mu_{b_1})}{R^+(p_1, \gamma_{p_1}\mu_{b_1}) R^+(p_2, \gamma_{p_2}\mu_{b_2})}, \quad (\text{E.2})$$

for the conditional δ -distributions, see Eqs.(D.4) and (D.5). In Eq.(E.1) we compare source fluxes provided $u \geq 0$. If $u < 0$, we simply exchange measurements, using $P(j_1 < j_2) = 1 - P(j_2 < j_1)$.

In a similar way and under the same conditions, we can compare two independent on-off measurements through the ratios β_1 and β_2 when background uncertainties are not considered. Using the parameter ξ , the probability of inconsistency between two ratios (see Eq.(14)) is written ($p_1, p_2 \in N$)

$$P(\beta_1 < \xi \beta_2) = \frac{w^{p_2}}{(1+w)^{p_1+p_2}} \sum_{k=1}^{p_2} \binom{p_1+p_2-k-1}{p_2-k} \left(\frac{1+w}{w}\right)^k R_k(w), \quad (\text{E.3})$$

where $w = \xi^{-1}(\gamma_{p_2} \mu_{b_2}) / (\gamma_{p_1} \mu_{b_1})$ and $R_k(w) = 1$ for the unconditional β -distributions (Eq.(D.2)) and for the conditional ones (Eqs.(D.4) and (D.5)) it is written in Eq.(E.2). The formula in Eq.(E.3) holds for $\xi \leq 1$. If $\xi > 1$, we use $P(\beta_1 < \xi \beta_2) = 1 - P(\beta_2 < \xi^{-1} \beta_1)$.

- [1] D.Nosek, J.Nosková, Nucl. Instrum. Methods A 820 (2016) 23.
- [2] M.L.Knoetig, Astrophys. J. 790 (2014) 106.
- [3] D.Casadei, Astrophys. J. 798 (2015) 5.
- [4] O.Helene, Nucl. Instrum. Methods 212 (1983) 319.
- [5] O.Helene, Nucl. Instrum. Methods 228 (1984) 120.

- [6] H.B.Prosper, Nucl. Instrum. Methods A 241 (1985) 236.
- [7] H.B.Prosper, Phys. Rev. 37 (1988) 1153.
- [8] S.Gillesen and H.L.Harney, Astron. Astrophys. 430 (2005) 355.
- [9] P.Gregory, Bayesian Logical Data Analysis for the Physical Sciences, Cambridge University Press, Cambridge, 2005 (Chapter 14).
- [10] S.S.Wilks, Ann. Math. Stat. 9 (1938) 60.
- [11] T.P.Li, Y.Q.Ma, Astrophys. J. 272 (1983) 317.
- [12] R.D.Cousins, Nucl. Instrum. Methods A 417 (1998) 391.
- [13] G.Cowan, K.Cranmer, E.Gross, O.Vitells, Eur. Phys. J. C71 (2011) 1554; G.Cowan, K.Cranmer, E.Gross, O.Vitells Eur. Phys. J. C73 (2013) 2501.
- [14] G.J.Feldman, R.D.Cousin, Phys. Rev. D57 (1998) 3873.
- [15] R.D.Cousins, J.T.Linnemann, J.Tucker, Nucl. Instrum. Methods A 595 (2008) 480.
- [16] W.A.Rolke, A.M.López, J.Conrad, Nucl. Instrum. Methods A 551 (2005) 493.
- [17] S.Algeri, J.Conrad, D.A.van Dyk, MNRAS 458 (2016) L84.
- [18] J.Abraham *et al.* (The Pierre Auger Collaboration), Science 318 (2007) 928.
- [19] J.Abraham *et al.* (The Pierre Auger Collaboration), Astropart. Phys. 29 (2008) 188.
- [20] P.Abreu *et al.* (The Pierre Auger Collaboration), Astropart. Phys. 34 (2010) 314.
- [21] P.Abreu *et al.* (The Pierre Auger Collaboration), JCAP 06 (2011) 022.
- [22] A.Aab *et al.* (The Pierre Auger Collaboration), Astrophys. J. 804 (2015) 15.

- [23] F.W.J.Olver, D.M.Lozier, R.F.Boisvert, C.W.Clark (eds.), NIST Handbook of Mathematical Functions, Cambridge University Press, Cambridge, 2010, (Chapters 8 and 13).
- [24] B.McDonald, *Econometrica* 52 (1984) 647.
- [25] T.Abu-Zayyad *et al.*, *Astrophys. J.* 757 (2012) 26.
- [26] T.Abu-Zayyad *et al.*, *Astrophys. J.* 777 (2013) 88.
- [27] H.C.Tijms, *A First Course in Stochastic Models*, John Wiley & Sons Ltd., Chichester, 2003, (Chapters 1).
- [28] N.L.Johnson, A.W.Kemp, S.Kotz, *Univariate Discrete Distributions*, John Wiley & Sons, Inc., Hoboken, 2005, (Chapters 5).
- [29] K.Kawata *et al.* (The Telescope Array Collaboration), *The 34th International Cosmic Ray Conference, 30 July-6 August 2015, the Hague, The Netherlands*.
- [30] M.-P.Véron-Cetty, P.Véron, *Astron. Astrophys.* 455 (2006) 773.
- [31] A.Aab *et al.* (The Pierre Auger Collaboration), *JCAP* 08 (2015) 049.